Atherosclerosis and Lipoproteins

Troglitazone Inhibits Formation of Early Atherosclerotic Lesions in Diabetic and Nondiabetic Low Density Lipoprotein Receptor–Deficient Mice

Alan R. Collins, Woerner P. Meehan, Ulrich Kintscher, Simon Jackson, Shu Wakino, Grace Noh, Wulf Palinski, Willa A. Hsueh, Ronald E. Law

Abstract—Peroxisome proliferator–activated receptor-γ (PPARγ) is a ligand-activated nuclear receptor expressed in all of the major cell types found in atherosclerotic lesions: monocytes/macrophages, endothelial cells, and smooth muscle cells. In vitro, PPARγ ligands inhibit cell proliferation and migration, 2 processes critical for vascular lesion formation. In contrast to these putative antiatherogenic activities, PPARγ has been shown in vitro to upregulate the CD36 scavenger receptor, which could promote foam cell formation. Thus, it is unclear what impact PPARγ activation will have on the development and progression of atherosclerosis. This issue is important because thiazolidinediones, which are ligands for PPARγ, have recently been approved for the treatment of type 2 diabetes, a state of accelerated atherosclerosis. We report herein that the PPARγ ligand, troglitazone, inhibited lesion formation in male low density lipoprotein receptor–deficient mice fed either a high-fat diet, which also induces type 2 diabetes, or a high-fructose diet. Troglitazone decreased the accumulation of macrophages in intimal xanthomas, consistent with our in vitro observation that troglitazone and another thiazolidinedione, rosiglitazone, inhibited monocyte chemoattractant protein-1–directed transendothelial migration of monocytes. Although troglitazone had some beneficial effects on metabolic risk factors (in particular, a reduction of insulin levels in the diabetic model), none of the systemic cardiovascular risk factors was consistently improved in either model. These observations suggest that the inhibition of early atherosclerotic lesion formation by troglitazone may result, at least in part, from direct effects of PPARγ activation in the artery wall. (*Arterioscler Thromb Vasc Biol.* 2001;21:365-371.)

Key Words: atherosclerosis ■ diabetes mellitus ■ pharmacology

Peroxisome proliferator–activated receptor-γ (PPARγ), a nuclear receptor, is expressed in all major cell types participating in vascular injury: endothelial cells (ECs), macrophages, and vascular smooth muscle cells (VSMCs).[1–6] Activation of this receptor in vitro inhibits inflammatory processes, including cytokine production and expression of NO synthase.[2] In early clinical investigations, ligands of PPARγ, such as thiazolidinediones (TZDs), have also been reported to improve endothelium-dependent vasodilation, suggesting that PPARγ activation enhances NO production and protects against vascular injury.[7,8] Activation of PPARγ also inhibits 2 other processes critical for vascular lesion formation, cell proliferation, and migration.[3,5,6,9,10] In vivo, 2 TZDs, troglitazone (TRO) and pioglitazone, significantly reduced arterial neointimal hyperplasia after endothelial injury in rats.[11–13] In such balloon-catheterized arteries, neointima formation essentially reflects increased migration and proliferation of VSMCs, a major contributor to the growth of

See page 295

atherosclerotic lesions. TRO also inhibited neointima formation in stents placed in the coronary arteries of patients with type 2 diabetes.[14]

We and others have recently demonstrated that PPARγ activation by TZDs and 15-deoxy-$\Delta^{12,14}$-prostaglandin J_2 inhibits EC expression of vascular cell adhesion molecule-1, which mediates monocyte adherence to the endothelial surface.[4,15] Because inflammation, dysregulated growth, and migration of monocytes and VSMCs play an important role in the development of atherosclerosis, we hypothesized that PPARγ activation in cells of the vasculature would inhibit the atherosclerotic process. On the other hand, TZDs also stimulate conversion of macrophages into foam cells; therefore, ligand-dependent activation of PPARγ has been postulated to promote atherosclerosis.[16]

Received August 10, 2000; revision accepted December 1, 2000.

From the Division of Endocrinology, Diabetes, and Hypertension (A.R.C., W.P.M., U.K., S.J., S.W., G.N., W.A.H., R.E.L.), Department of Medicine, UCLA School of Medicine, Los Angeles, Calif; the Molecular Biology Institute (W.A.H., R.E.L.), Los Angeles, Calif; the Department of Medicine/Cardiology (U.K.), Virchow-Klinikum, Humboldt University, and the German Heart Institute (U.K.), Berlin, Germany; and the Department of Medicine (W.P.), UCSD, La Jolla, Calif.

Correspondence to Ronald E. Law, PhD, University of California, Los Angeles, Division of Endocrinology, Diabetes, and Hypertension, 900 Veteran Ave, Suite 24-130, Box 957073, Los Angeles, CA 90095. E-mail rlaw@mednet.ucla.edu

Arterioscler Thromb Vasc Biol. is available at http://www.atvbaha.org

The impact of TZDs on atherosclerosis is a critical issue. TZDs improve insulin-mediated glucose uptake and are used extensively in the treatment of insulin resistance and type 2 diabetes mellitus.[17] Coronary artery disease mortality is increased 2- to 4-fold in type 2 diabetes.[18] Atherosclerosis is the major cause of demise in people with diabetes; therefore, it is important to determine the action of any antidiabetic drug on the atherosclerotic process.

To determine whether PPARγ activation has proatherogenic or antiatherogenic effects, we administered TRO to male LDL receptor–deficient ($LDLR^{-/-}$) mice fed either a high-fat or a high-fructose atherogenic diet. Both models develop substantial hypercholesterolemia and macrophage-laden lesions, designated intimal xanthomata, which do not normally progress to mature atherosclerotic plaques.[19] In addition, the high-fat diet induces hyperglycemia and hyperinsulinemia in the $LDLR^{-/-}$ mouse, making it also a model of type 2 diabetes.[20,21] In contrast, fructose does not increase glucose or insulin in this model[21] and, therefore, was useful because the effects of TZDs on atherosclerosis could be studied in the absence of improvements in insulin action.

Methods

Transendothelial Monocyte Migration

THP-1 cells (5×10^4), a human monocytic leukemia cell line, were added to a human aortic EC monolayer covering a gelatin-coated 8-μm porous membrane and incubated for 30 minutes at 37°C to facilitate their attachment. Cells were then pretreated with the indicated ligands or vehicle (dimethyl sulfoxide) for 30 minutes at 37°C. Migration was induced by the addition of monocyte chemoattractant protein-1 (MCP-1, 50 ng/mL) to the lower compartment. After 90 minutes, nonmigrating THP-1 cells and human aortic ECs were removed with a cotton tip, and the membranes were fixed and stained with the Quik-Diff Stain Set (DADE, Miami, Fla) to identify migrated cells. The number of migrated cells was determined per ×320 high-power field. Experiments were performed in duplicate and were repeated at least 3 times.

Western Blots

Western immunoblots were performed as previously described.[10] Membranes were incubated with rabbit polyclonal antibodies (1:1000 dilution, New England Biolabs) that recognize either (1) total extracellular signal–regulated kinase (ERK) or (2) ERK phosphorylated on threonine 202 and tyrosine 204.

Animals and Diets

Male $LDLR^{-/-}$ mice were obtained (C57BL/6J-$Ldlr^{tm1Her}$, stock No. 002207, Jackson Laboratory, Bar Harbor, Me) and were group-housed under a 12-hour light and 12-hour dark regimen. All animal protocols were approved by the UCLA Animal Research Committee and complied with all federal, state, and institutional regulations. At 3 months of age, the mice were randomly assigned to 1 of 5 dietary regimens: (1) chow (Harlan Teklad 8604), (2) high-fat complex carbohydrate (Research Diets), (3) high-fat complex carbohydrate with 4 g TRO/kg of food, (4) high fructose (Research Diets), or (5) high fructose with 4 g TRO/kg of food. The high-fat diet consisted of 21% fat, 20% protein, 50% carbohydrate, and 0.15% cholesterol. Our high-fat diet differed from those commonly used to study atherogenesis in $LDLR^{-/-}$ mice in that the majority of the nonfat energy came from complex carbohydrate sources instead of sucrose. The high-fructose diet contained 4% fat, 16% protein, 71% fructose, and 0.15% cholesterol. Sources of fat in the diets were corn oil (1% in all diets) and anhydrous milk fat (3% in the fructose diets and 20% in the high fat diets). Mice and feed were weighed weekly, and the rate of consumption of drug was computed. The mice were fed for a period of 12 weeks.

Metabolic Measurements

Blood samples from the retro-orbital sinus were obtained from the mice before the beginning of treatment and every month thereafter and from the abdominal vena cava at euthanasia. Mice were fasted overnight before the collection of the blood samples. Plasma glucose was measured by glucose oxidase reaction (Beckman Glucose Analyzer 2, Beckman Instruments). Plasma lipids were measured by the UCLA Lipid Analysis Laboratory. Plasma insulin was determined by ELISA. Blood pressures were obtained by using an indirect tail-cuff method with a controlled temperature chamber (ITC, Inc) by a technician blinded to the treatment groups.

Vessel Preparation and Image Analysis

Mice were euthanized and perfused with 7.5% sucrose in 4% paraformaldehyde. Aortas were dissected out, split longitudinally, pinned flat in a dissection pan, and stained with Sudan IV to detect lipids and determine lesion area. Images were captured by use of a Sony 3-CCD video camera and analyzed by a single technician who was blinded to the study protocol and used ImagePro image analysis software. The extent of lesion formation is expressed as the percentage of the total aortic surface area covered by lesions.

Cross Sections: Determination of Intimal Macrophage Content

The largest lesions from the aortic arch were excised and embedded in paraffin. The avidin-biotin-peroxidase complex technique for immunostaining was used. Macrophages were stained by using monoclonal antibody to CD68 (titer 1:100, KP1 clone, M0814, Dako Corp). Nonimmune serum was used as a control. Primary antibody incubations were performed in 1% BSA/2% goat serum containing PBS for 60 minutes. Biotinylated rabbit anti-mouse (Dako) was applied; incubation with a streptavidin-peroxidase complex followed. Peroxidase activity was detected with the use of diaminobenzidine tetrahydrochloride as a chromogen. Slides were then counterstained with hematoxylin. Images of the stained sections were analyzed by using the software described above. After tracing the intimal area to be measured with a cursor, 5 pixels of color, which defined the anti-CD68 stain, were sampled by the operator. The area encompassed by the pixels, which was not contiguous, in the color range for anti-CD68 was then computed automatically by the software. This approach has been successfully used by Shi et al[22] to quantify lesional macrophages in a mouse model of transplant arteriosclerosis.

Statistical Analysis

Statistical analysis was performed by using 2-factorial ANOVA with Student-Newman-Keuls to determine the differences between individual group means.

Results

TRO Inhibits Monocyte Migration

VSMC migration and proliferation play an important atherogenic role in the progression of fatty streaks toward more advanced atherosclerotic lesions, such as transitional lesions and classical atheromas. We have previously shown that PPARγ ligands inhibit ERK mitogen-activated protein kinase (MAPK)-dependent migration of VSMCs.[10,11] However, in the earliest stages of atherosclerotic lesions, recruitment of adherent monocytes through their migration into the subendothelium and their phenotypic transformation to macrophages and foam cells play a far greater role than VSMCs in humans and in murine models.[23]

To investigate whether TRO-mediated PPARγ activation affects monocyte recruitment and to further explore its mechanism, we carried out a series of in vitro experiments before our in vivo studies. MCP-1 is an important in vivo migration factor promoting the subendothelial accumulation of monocytes. TRO inhibited MCP-1–directed transmigra-

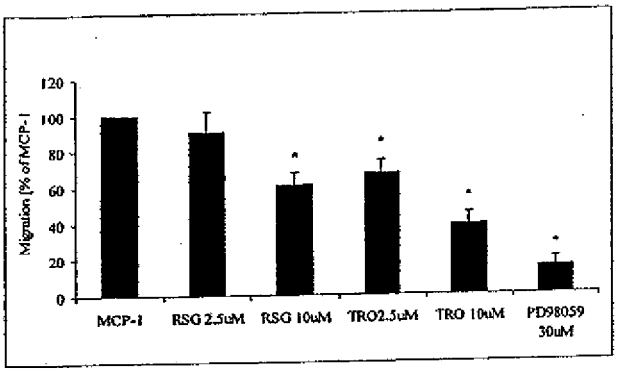

Figure 1. PPARγ ligands inhibit MCP-1–directed transendothelial migration of monocytes. Migration of THP-1 monocytes through ECs was determined by using a modified Boyden chamber assay as described in Methods. The number of migrating cells was quantified by microscopy with the use of high-power fields. Results represent 3 independent experiments performed in duplicate. *$P<0.05$ vs MCP-1 alone.

tion of THP-1 monocytes by 32.7±6.5% at 2.5 μmol/L and by 61.4±6.7% at 10 μmol/L (Figure 1). TRO contains a vitamin E moiety that may confer an antioxidant activity that can inhibit monocyte recruitment and endothelial expression of adhesion molecules. However, rosiglitazone (RSG), another PPARγ ligand that lacks antioxidant activity, also inhibited monocyte transmigration, albeit with a lesser potency than TRO (Figure 1). Inhibition of monocyte transmigration by TRO, therefore, is likely to be mediated at least in part through PPARγ.

MCP-1 rapidly induced ERK activation, reaching a peak at 5 minutes, which was blocked by PD98059, an inhibitor of MAPK ERK kinase (MEK, an upstream kinase), which phosphorylates and activates ERK (Figure 2). PD98059 attenuated MCP-1–directed transmigration by 84.8±4.8%. In combination, these data suggest that activation of PPARγ in monocytes may inhibit their migration by interfering with ERK-MAPK signaling, although the precise mechanism remains to be determined.

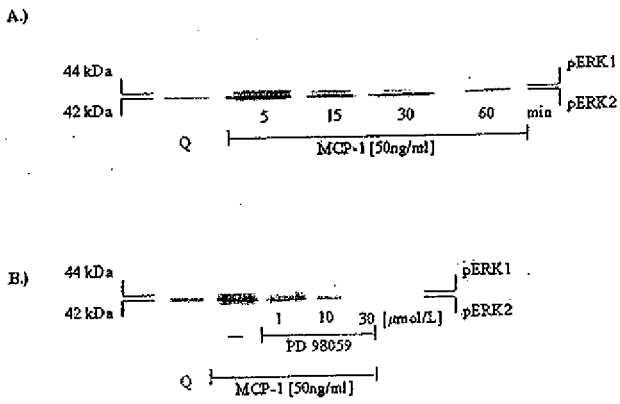

Figure 2. MCP-1 activates the ERK-MAPK pathway in THP-1 human monocytes. A, Quiescent (Q) THP-1 cells were stimulated with MCP-1 (50 ng/mL) for 5 minutes. Whole-cell protein extracts were immunoblotted with a phosphospecific ERK1 (pERK1)/ERK2 (pERK2) MAPK antibody. A representative blot of 3 different experiments is shown. B, Conditions were the same as in panel A except that cells were treated with MEK inhibitor PD98059 (1 to 30 μmol/L) or vehicle (dimethyl sulfoxide, −) before and during stimulation with MCP-1 (50 ng/mL). A representative blot of 3 different experiments is shown.

TRO Inhibits Intimal Macrophage Accumulation and Lesion Formation in Male LDLR$^{-/-}$ Mice

LDLR$^{-/-}$ mice that were fed a regular chow diet develop few lesions across the surface of the aorta. Male 3-month-old LDLR$^{-/-}$ mice were placed on either a high-fat or high-fructose diet to induce atherosclerosis. LDLR$^{-/-}$ males were used in the present study because they develop hyperglycemia and become diabetic on a high-fat diet but remain normoglycemic when fed a high-fructose diet. Moreover, males develop twice the level of surface lesions as do females,[24] and their use obviates the potentially confounding influence of the vascular protection in females afforded by estrogen. Comparison of the impact of TRO on atherogenesis in these 2 dietary models was undertaken to distinguish any activity of PPARγ to normalize metabolic abnormalities accompanying diabetes that contribute to high-fat–induced xanthomata formation from any direct effects on the vasculature. To assess the impact of TRO on aortic lesions, 1 high-fat diet group and 1 high-fructose diet group received TRO at 400 mg/kg body wt per day from drugs pelleted into the atherogenic diets. This dose of TRO was chosen because we previously demonstrated its efficacy in inhibiting intimal hyperplasia in rats after balloon injury.[11]

The en face method, which makes use of computer-assisted analysis of color images of Sudan IV–stained lipid-containing material in the entire aorta, was used to determine the percentage of surface area affected by lesions.[24] Male LDLR$^{-/-}$ mice on normal chow for 3 months had <0.20% lesions (Figure 3A). The high-fat diet increased the amount of surface lesions after 3 months to 3.90±0.16% (n=8, Figure 3B). TRO inhibited the high-fat–induced lesions by 30% (2.76±0.36% of the aortic surface, n=8, $P<0.02$; Figure 3C). Similar to Merat et al,[21] we noted that the high-fructose diet was more atherogenic than the high-fat diet, causing 8.42±0.94% lesions (n=17, Figure 3D). TRO reduced lesions in fructose-fed LDLR$^{-/-}$ males by 42% (4.90±0.65%, n=14, $P<0.01$; Figure 3E). Quantitative results are summarized in Figure 4.

TRO-treated male LDLR$^{-/-}$ mice fed either the high-fat or high-fructose diet for 3 months developed lesions that contained substantially fewer CD68-staining macrophages (Figure 5A through 5D). Lesions induced by a high-fat diet contained 39.1±6.8% macrophages (percent of cross-sectional intimal area) compared with 13.3±4.9% ($P<0.01$) in mice administered TRO (Figure 5E). Similar results were obtained for males fed the high-fructose diet, where TRO decreased macrophage accumulation from 40.4±3.5% to 17.1±1.7% ($P<0.01$, Figure 5E). The lesions in the TRO-fed animals tended to be smaller in volume than those in males not fed TRO. The relative macrophage content in the larger lesions (not treated with TRO) exceeded the content in the smaller lesions (treated with TRO) by 140% to 200%. The reduction in macrophage accumulation in the lesions of TRO-treated animals is unlikely to be the result of their being an earlier lesion stage, because the relative macrophage content is known to be greatest in the smaller (ie, early-stage) lesions.

Effect of TRO on Metabolic Parameters

All metabolic measurements determined on blood samples drawn before treatment were similar in all groups (Tables 1

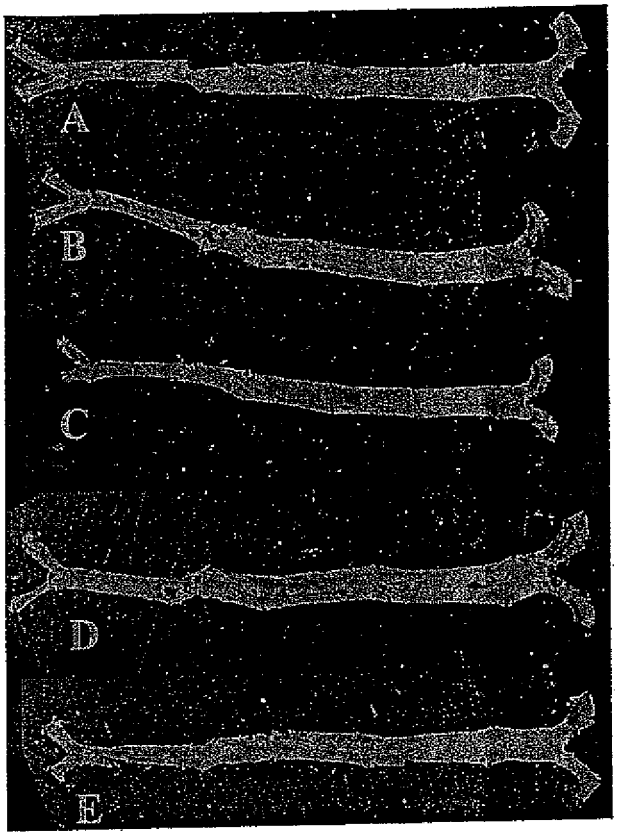

Figure 3. TRO attenuates atherosclerosis in male LDLR$^{-/-}$ mice. The aorta is stained by Sudan IV to detect the lipids present in lesions. A, Chow diet. B, High-fat diet. C, High-fat diet and TRO. D, High-fructose diet. E, High-fructose diet and TRO.

and 2). In accordance with previous studies on male LDLR$^{-/-}$ mice, we found that a high-fat diet induced diabetes[20,21] (Table 1). Glucose levels progressively increased throughout

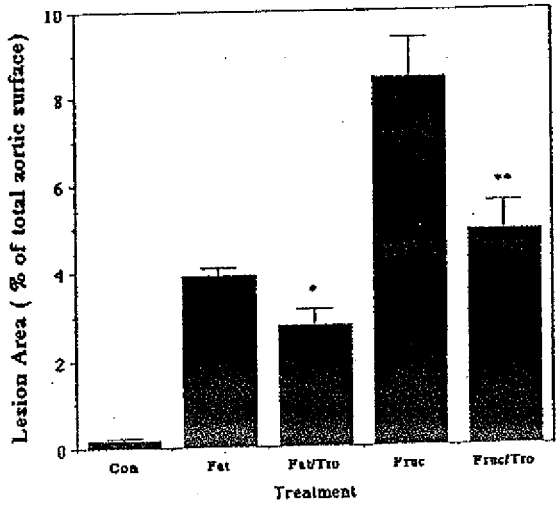

Figure 4. Quantification of the antiatherogenic activity of TRO in male LDLR$^{-/-}$ mice. Mean atherosclerotic surface lesion areas were determined in mice fed a normal chow, high-fat, or high-fructose diet in the absence or presence of TRO for 3 months. Image analysis and quantification of the percentage of the total aortic area staining for Sudan IV were performed by using computer-assisted image analysis. TRO produced a significant decrease in mice fed a high-fat (30% decrease, $^{*}P<0.05$) and high-fructose (42% decrease, $^{**}P<0.05$) diet.

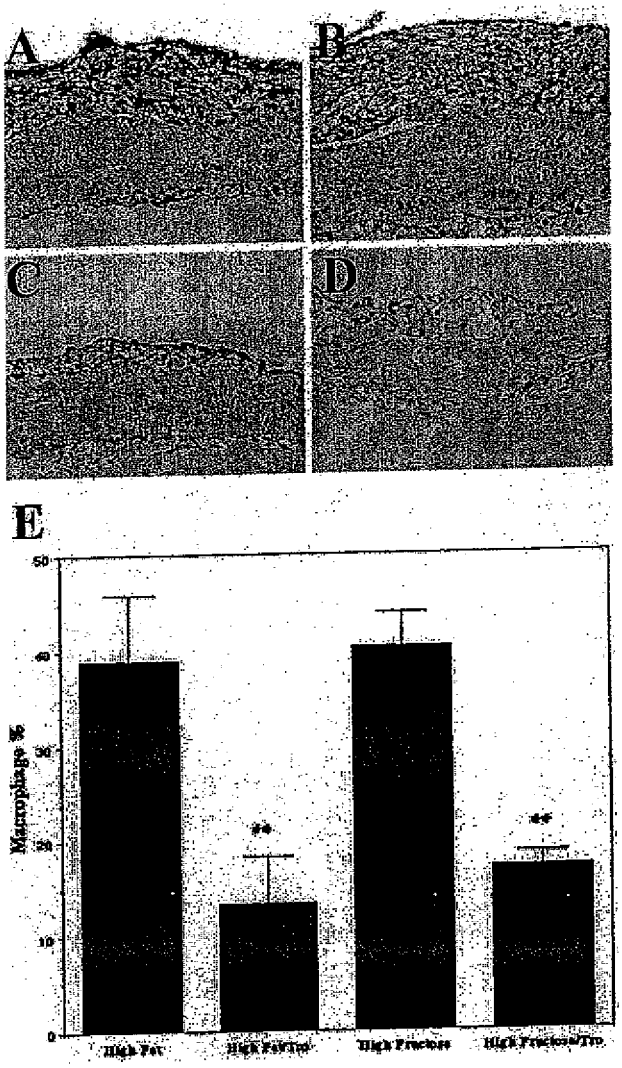

Figure 5. TRO inhibits accumulation of lesional macrophages. Sections from the aortic arch were immunostained by using antibody against CD68 to detect macrophages. Quantification of the percentage of the intimal area staining ($^{**}P<0.05$) for CD68 was performed by computer-assisted image analysis. A, High-fat diet (n=6). B, High-fat diet and TRO (n=6). C, High-fructose diet (n=6). D, High-fructose diet and TRO (n=6). E, Quantification of the macrophage content.

the study, reaching a maximum of 285 mg/dL at 3 months compared with 148 mg/dL for mice on normal chow. The fat-fed males were also hyperinsulinemic (1198±149 versus 664±113 pg/mL on normal chow), consistent with the development of early-stage type II diabetes. Although TRO did not decrease hyperglycemia in high-fat–fed male mice, TRO administration completely normalized their plasma insulin levels. In marked contrast, mice on a high-fructose diet had normal fasting plasma glucose and insulin levels, which were not altered by TRO.

LDLR$^{-/-}$ males developed severe hypercholesterolemia on either the high-fat or high-fructose diet, achieving levels 3- to 4-fold greater than those in animals maintained on regular chow (Table 2). TRO lowered total plasma cholesterol by 27% in males on the high-fructose diet but had no effect on the high-fat–fed mice. Triglycerides were elevated in the high-fat–fed males but not in the high-fructose group; TRO

TABLE 1. Plasma Glucose and Insulin Levels and Final Body Weights

	Chow Diet	High-Fat Diet	High-Fat Diet/TRO	High-Fructose Diet	High-Fructose Diet/TRO
Glucose, mg/dL					
Start	158.7±14.63	173.2±12.12	169.4±7.98	137.8±11.53	148.5±27.67
1 mo	148.9±6.60	190.5±10.92	155.1±9.13*	121.2±6.44	114.8±4.55
2 mo	144.8±10.96	201.1±9.09	189.6±27.37	128.6±13.09	121.89±17.32
3 mo	148.5±14.87	284.8±25.00	268.9±13.90	152.3±15.80	181.9±23.47
Insulin, pg/mL					
3 mo	664.7±113.62	1198.7±149.81	691.2±109.14†	304.4±47.49	278.7±37.9
Body weight, g	27.3±0.56	42.5±0.66	37.0±0.89†	25.9±0.37	24.2±0.34

Values are mean±SEM.
*$P<0.05$ vs high-fat; †$P<0.01$ vs high-fat diet.

did not alter triglycerides in either model. HDL cholesterol (HDLC) decreased with both of the diets, compared with normal chow, as frequently reported.[3] TRO further lowered the HDLC in the high-fat–fed males but increased it in the high-fructose–fed group. Plasma free fatty acid levels increased in males on the high-fat diet but not in those on the high-fructose diet; TRO decreased free fatty acid levels in both models.

Discussion

The most significant finding of the present study is that TRO inhibited lesion formation in a type 2 diabetic mouse model and a nondiabetic LDLR$^{-/-}$ mouse model of intimal xanthomata. Mice fed the high-fat diet developed extensive hypercholesterolemia that was not affected by TRO. These mice also gained substantial weight and showed an increase in circulating free fatty acid levels, which probably contributed to their insulin resistance, hyperinsulinemia, and fasting hyperglycemia.[25] The increase in triglycerides and decrease in HDLC are consistent with insulin resistance. TRO decreased circulating insulin but did not affect glucose in this model. The same has been reported in humans with type 2 diabetes, of whom 20% treated with TRO showed no improvement in glucose control, but all demonstrated improved insulin sensitivity.[26] In contrast to the response in humans, TRO did not alter triglycerides and further decreased HDLC. Mice fed the high-fructose diet also developed severe hypercholesterolemia but did not gain weight or develop hyperinsulinemia or elevations in free fatty acids or triglycerides. In this model, TRO decreased the free fatty acids, increased HDLC, and decreased total cholesterol.

TABLE 2. Plasma Lipid Levels

	Chow Diet	High-Fat Diet	High-Fat Diet/TRO	High-Fructose Diet	High-Fructose Diet/TRO
Total Cholesterol, mg/dL					
Start	292.2±14.63	277.7±5.77	278.8±9.24	321.8±20.87	328.0±18.32
1 mo	316.0±11.51	583.3±72.18	541.9±62.22	489.1±24.58	360.8±21.37†
2 mo	315.8±10.26	1307.0±110.11	1173.0±122.11	1052.3±33.78	816.7±25.02‡
3 mo/final	317.9±17.79	1341.9±52.14	1313.63±28.83	1167.7±46.17	862.1±23.70‡
HDLC, mg/dL					
Start	110.6±4.51	111.2±1.87	109.9±3.07	121.2±2.59	113.5±8.39
1 mo	111.2±3.19	108.2±1.93	108.9±2.65	104.2±3.08	106.6±4.58
2 mo	112.1±4.06	94.4±3.52	98.2±12.66	100.4±3.56	105.3±4.76
3 mo	112.4±5.00	104.8±7.84	81.8±6.86*	90.1±4.48	108.4±5.10†
Free fatty acids, mg/dL					
Start	67.1±2.82	63.5±1.82	58.2±2.67	91.0±6.96	82.5±4.38
1 mo	69.4±2.97	70.4±2.11	66.6±2.67	66.9±4.90	71.2±3.75
2 mo	65.7±2.87	88.6±7.32	74.2±4.19	68.7±3.67	65.8±3.57
3 mo	61.7±3.68	72.5±2.42	57.1±2.07*	61.7±1.52	53.1±2.81†
Triglycerides, mg/dL					
Start	122.0±4.43	109.1±5.32	101.1±5.72	84.8±5.09	111.83±16.00
1 mo	126.0±11.1	124.3±7.00	113.6±7.48	85.8±4.98	94.0±6.47
2 mo	86.9±4.98	156.6±30.55	191.8±64.47	81.2±5.98	79.8±6.47
3 mo	71.6±6.92	141.8±7.84	159.1±19.79	75.3±6.89	69.0±4.85

Values are mean±SEM.
*$P<0.01$ vs high-fat diet; †$P<0.05$ vs high-fructose diet, and ‡$P<0.001$ vs high-fructose diet.

Despite the difference in metabolic responses between the diabetic and nondiabetic animals, both hypercholesterolemic models responded to TRO with decreased lesion formation. These results suggest that TRO has direct vascular effects, separate from its metabolic effects, that decrease the atherosclerotic process. Alternatively, the antiatherogenic effects of TRO in the 2 different models might involve the collection of distinct metabolic processes. For example, hemodynamic effects of TRO related to its reported activity to lower blood pressure in animal models and in humans could also impact pathophysiological processes in high-fat– and high-fructose–fed LDLR$^{-/-}$ mice.[27–30] All major cell types contributing to this vascular lesion formation express PPARγ, which provides a mechanism for the direct effect of thiazolidinedione ligands in the vessel wall.[3,5,6,9] Data from in vitro experiments had suggested mechanisms by which activation of PPARγ could either accelerate or attenuate the atherosclerotic process.[2–6,9,10,16] The present study provides conclusive evidence that ligand-induced PPARγ activation by TRO reduces intimal xanthomata in murine models.

TRO had several systemic effects that may have contributed to its attenuation of intimal xanthomata. In the diabetic high-fat–fed mouse, TRO lowered insulin and glucose levels and decreased HDLC (which is thought to promote atherogenesis). In the fructose-fed model, TRO decreased total cholesterol and increased HDLC. Our finding that TRO was more potent in suppressing lesion formation in the fructose-fed model compared with the high-fat–fed mice could be due to the observed 27% reduction in total cholesterol. A common effect of TRO in the high-fat–fed and high-fructose–fed LDLR$^{-/-}$ models is its suppression of circulating free fatty acid levels. However, increased circulating free fatty acids have not been shown to be an independent risk factor for atherosclerosis.

Inflammation in the vascular wall has clearly emerged as a major culprit in the development of atherosclerosis.[31] Damage to the endothelium and the subsequent recruitment and transendothelial migration of monocytes constitute critical early cellular responses during atherogenesis.[31] Transmigration of monocytes into the subendothelial space is strongly stimulated by the chemokine MCP-1, which is expressed and secreted by ECs and VSMCs. The essential role of MCP-1 in atherogenesis is underscored by a recent study demonstrating that crossing MCP-1–deficient mice into LDLR$^{-/-}$ mice attenuated lesion formation by >80%.[32] Our group and others have shown that TRO and other PPARγ ligands inhibit growth factor–directed ERK-MAPK–dependent VSMC migration.[5,10,11] Cell migration requires de novo gene transcription that is consistent with PPARγ acting in the nucleus to inhibit this process.[10] In particular, activation of PPARγ can inhibit ERK-MAPK signaling to the nucleus.[11,33] Because MCP-1–directed migration of monocytes is ERK-MAPK dependent, interference with this pathway by TRO could contribute to the observed reduction in intimal xanthomata and lesional macrophages in treated LDLR$^{-/-}$ mice.

TRO and another PPARγ ligand, RSG, which does not contain an α-tocopherol moiety, inhibited MCP-1–directed migration of human monocytes in vitro. TRO also consistently decreased intimal macrophage accumulation in the diabetic and nondiabetic mice. These findings support the concept that inhibition of monocyte attachment and migration in the vessel by TRO may be one of the mechanisms contributing to the reduction of atherogenesis. Although it cannot be ruled out that the reduction of intimal monocytes in part reflected the reduced lesion size induced by TRO treatment, this is unlikely to be the sole explanation, because the relative intimal monocyte/macrophage content is known to be greatest in the early stages (smaller lesions) of atherosclerosis. In any case, the antiatherosclerotic activity of TRO-induced PPARγ activation clearly prevailed over its hypothesized promotion of foam cell formation via increased expression of the scavenger receptor CD36.[16]

Unlike other PPARγ ligands, TRO has an α-tocopherol (vitamin E) moiety that theoretically could contribute to its antiatherogenic activity through antioxidant effects.[34] Vitamin E has been shown to suppress atherosclerosis in the apoE knockout model, which develops advanced atherosclerotic lesions.[35,36] Whether the dose of vitamin E provided by TRO in the present study is enough to impact lesion formation is doubtful. At 400 mg/kg TRO per day, LDLR$^{-/-}$ mice received the equivalent of 8 IU of vitamin E, a dose much lower than that reported to affect atherosclerosis or to significantly protect LDL against oxidation.[35–38] Another line of evidence for the assumption that the effect of TRO on lesion formation was not, to a significant degree, dependent on antioxidant effects is provided by a parallel study demonstrating that 2 other PPARγ ligands, RSG and GW7845,which do not contain the α-tocopherol moiety, inhibited atherogenesis in the aortic root of male LDLR$^{-/-}$ mice fed a high-fat, cholesterol-enriched diet.[39] In addition, the recent Heart Outcomes Prevention Evaluation (HOPE) clinical trial in humans did not show an effect of vitamin E on coronary artery disease events or mortality.[40]

In summary, given the absence of consistent major metabolic changes present in diabetic and nondiabetic mice, it is likely that TRO at least in part decreases early atherosclerotic lesion formation through direct vascular effects. In human subjects with diabetes, who have a high risk for coronary disease, TRO improves insulin resistance and other proatherogenic metabolic parameters, which may improve cardiovascular risk. It is possible that some of the vascular effects observed in our murine models may also be present in humans. Although Li et al[39] and our data demonstrate that PPARγ ligands suppress early atherosclerotic lesions, intimal xanthomata do not inexorably progress to more advanced atherosclerotic plaques; in fact, they often regress.[19] Therefore, determining the effects of PPARγ ligands on more advanced atherosclerotic lesions may prove to be a stronger predictor of their potential clinical benefit. Nonetheless, the present results indicate that an investigation of potential antiatherogenic effects of PPARγ ligands is strongly warranted.

Acknowledgments

This work was supported by National Institutes of Health grant HL-58328 to Willa A. Hsueh. Shu Wakino was supported by a Mary K. Iacocca Fellowship in Diabetes. Ulrich Kintscher was supported by a Gonda (Goldschmeid) Fellowship in Diabetes.

References

1. Ricote M, Huang J, Fajas L, Li A, Welch J, Najib J, Witztum JL, Auwerx J, Palinski W, Glass CK. Expression of the peroxisome proliferator-activated receptor gamma (PPARgamma) in human atherosclerosis and

regulation in macrophages by colony stimulating factors and oxidized low density lipoprotein. *Proc Natl Acad Sci U S A.* 1998;95:7614–7619.
2. Ricote M, Li AC, Willson TM, Kelly CJ, Glass CK. The peroxisome proliferator-activated receptor-gamma is a negative regulator of macrophage activation. *Nature.* 1998;391:79–82.
3. Xin X, Yang S, Kowalski J, Gerritsen ME. Peroxisome proliferator-activated receptor gamma ligands are potent inhibitors of angiogenesis in vitro and in vivo. *J Biol Chem.* 1999;274:9116–9121.
4. Jackson SM, Parhami F, Xi XP, Berliner JA, Hsueh WA, Law RE, Demer LL. Peroxisome proliferator-activated receptor activators target human endothelial cells to inhibit leukocyte-endothelial cell interaction. *Arterioscler Thromb Vasc Biol.* 1999;19:2094–2104.
5. Marx N, Schonbeck U, Lazar MA, Libby P, Plutzky J. Peroxisome proliferator-activated receptor gamma activators inhibit gene expression and migration in human vascular smooth muscle cells. *Circ Res.* 1998; 83:1097–1103.
6. Law RE, Goetze S, Xi XP, Jackson S, Kawano Y, Demer L, Fishbein MC, Meehan WP, Hsueh WA. Expression and function of PPARgamma in rat and human vascular smooth muscle cells. *Circulation.* 2000;101: 1311–1318.
7. Tack CJ, Ong MK, Lutterman JA, Smits P. Insulin-induced vasodilatation and endothelial function in obesity/insulin resistance: effects of troglitazone. *Diabetologia.* 1998;41:569–576.
8. Murakami T, Mizuno S, Ohsato K, Moriuchi I, Arai Y, Nio Y, Kaku B, Takahashi Y, Ohnaka M. Effects of troglitazone on frequency of coronary vasospastic-induced angina pectoris in patients with diabetes mellitus. *Am J Cardiol.* 1999;84:92–94. A8. Abstract.
9. Tanaka T, Itoh H, Do KK, Fukunaga Y, Arai H, Hosoda K. Activation of PPARgamma inhibits macrophage proliferation and migration: possible therapeutic effectiveness of thiazolidinediones on diabetic vascular complications. *Diabetes.* 1999;48(suppl 1):A30. Abstract.
10. Goetze S, Xi XP, Kawano H, Gotlibowski T, Fleck E, Hsueh WA, Law RE. PPAR gamma-ligands inhibit migration mediated by multiple chemoattractants in vascular smooth muscle cells. *J Cardiovasc Pharmacol.* 1999;33:798–806.
11. Law RE, Meehan WP, Xi XP, Graf K, Wuthrich DA, Coats W, Faxon D, Hsueh WA. Troglitazone inhibits vascular smooth muscle cell growth and intimal hyperplasia. *J Clin Invest.* 1996;98:1897–1905.
12. Igarashi M, Takeda Y, Ishibashi N, Takahashi K, Mori S, Tominaga M, Saito Y. Pioglitazone reduces smooth muscle cell density of rat carotid arterial intima induced by balloon catheterization. *Horm Metab Res.* 1997;29:444–449.
13. Yoshimoto T, Naruse M, Shizume H, Naruse K, Tanabe A, Tanaka M, Tago K, Irie K, Muraki T, Demura H, et al. Vasculo-protective effects of insulin sensitizing agent pioglitazone in neointimal thickening and hypertensive vascular hypertrophy. *Atherosclerosis.* 1999;145:333–340.
14. Takagi T, Akasaka T, Yamamuro A, Honda Y, Hozumi T, Morioka S, Yoshida K. Troglitazone reduces neointimal tissue proliferation after coronary stent implantation in patients with non-insulin dependent diabetes mellitus: a serial intravascular ultrasound study. *J Am Coll Cardiol.* 2000;36:1529–1535.
15. Pasceri V, Wu HD, Willerson JT, Yeh ET. Modulation of vascular inflammation in vitro and in vivo by peroxisome proliferator-activated receptor-gamma activators. *Circulation.* 2000;101:235–238.
16. Tontonoz P, Nagy L, Alvarez JG, Thomazy VA, Evans RM. PPARgamma promotes monocyte/macrophage differentiation and uptake of oxidized LDL. *Cell.* 1998;93:241–252.
17. Saltiel AR, Olefsky JM. Thiazolidinediones in the treatment of insulin resistance and type II diabetes. *Diabetes.* 1996;45:1661–1669.
18. Savage PJ. Cardiovascular complications of diabetes mellitus: what we know and what we need to know about their prevention. *Ann Intern Med.* 1996;124:123–126.
19. Virmani R, Kolodgie FD, Burke AP, Farb A, Schwartz SM. Lessons from sudden coronary death: a comprehensive morphological classification scheme for atherosclerotic lesions. *Arterioscler Thromb Vasc Biol.* 2000;20:1262–1275.
20. Towler DA, Bidder M, Latifi T, Coleman T, Semenkovich CF. Diet-induced diabetes activates an osteogenic gene regulatory program in the aortas of low density lipoprotein receptor-deficient mice. *J Biol Chem.* 1998;273:30427–30434.
21. Merat S, Casanada F, Sutphin M, Palinski W, Reaven PD. Western-type diets induce insulin resistance and hyperinsulinemia in LDL receptor–deficient mice but do not increase aortic atherosclerosis compared with normoinsulinemic mice in which similar plasma cholesterol levels are achieved by a fructose-rich diet. *Arterioscler Thromb Vasc Biol.* 1999; 19:1223–1230.
22. Shi C, Lee WS, Russell ME, Zhang D, Fletcher DL, Newell JB, Haber E. Hypercholesterolemia exacerbates transplant arteriosclerosis via increased neointimal smooth muscle cell accumulation: studies in apolipoprotein E knockout mice. *Circulation.* 1997;96:2722–2728.
23. Nakashima Y, Plump AS, Raines EW, Breslow JL, Ross R. ApoE-deficient mice develop lesions of all phases of atherosclerosis throughout the arterial tree. *Arterioscler Thromb.* 1994;14:133–140.
24. Tangirala RK, Rubin EM, Palinski W. Quantitation of atherosclerosis in murine models: correlation between lesions in the aortic origin and in the entire aorta, and differences in the extent of lesions between sexes in LDL receptor-deficient and apolipoprotein E-deficient mice. *J Lipid Res.* 1995;36:2320–2328.
25. Kelley DE, Goodpaster B, Wing RR, Simoneau JA. Skeletal muscle fatty acid metabolism in association with insulin resistance, obesity, and weight loss. *Am J Physiol.* 1999;277:E1130–E1141.
26. Suter SL, Nolan JJ, Wallace P, Gumbiner B, Olefsky JM. Metabolic effects of new oral hypoglycemic agent CS-045 in NIDDM subjects. *Diabetes Care.* 1992;15:193–203.
27. Fujiwara K, Hayashi K, Matsuda H, Kubota E, Honda M, Ozawa Y, Saruta T. Altered pressure-natriuresis in obese Zucker rats. *Hypertension.* 1999;33:1470–1475.
28. Sung BH, Izzo JL Jr, Dandona P, Wilson MF. Vasodilatory effects of troglitazone improve blood pressure at rest and during mental stress in type 2 diabetes mellitus. *Hypertension.* 1999;34:83–88.
29. Kawai T, Takei I, Oguma Y, Ohashi N, Tokui M, Oguchi S, Katsukawa F, Hirose H, Shimada A, Watanabe K, et al. Effects of troglitazone on fat distribution in the treatment of male type 2 diabetes. *Metabolism.* 1999;48:1102–1107.
30. Chen S, Noguchi Y, Izumida T, Tatebe J, Katayama S. A comparison of the hypotensive and hypoglycaemic actions of an angiotensin converting enzyme inhibitor, an AT1a antagonist and troglitazone. *J Hypertens.* 1996;14:1325–1330.
31. Ross R. Atherosclerosis is an inflammatory disease. *Am Heart J.* 1999; 138:S419–S420.
32. Gu L, Okada Y, Clinton SK, Gerard C, Sukhova GK, Libby P, Rollins BJ. Absence of monocyte chemoattractant protein-1 reduces atherosclerosis in low density lipoprotein receptor-deficient mice. *Mol Cell.* 1998; 2:275–281.
33. Goetze S, Xi XP, Graf K, Fleck E, Hsueh WA, Law RE. Troglitazone inhibits angiotensin II-induced extracellular signal-regulated kinase 1/2 nuclear translocation and activation in vascular smooth muscle cells. *FEBS Lett.* 1999;452:277–282.
34. Inoue I, Katayama S, Takahashi K, Negishi K, Miyazaki T, Sonoda M, Komoda T. Troglitazone has a scavenging effect on reactive oxygen species. *Biochem Biophys Res Commun.* 1997;235:113–116.
35. Shaish A, George J, Gilburd B, Keren P, Levkovitz H, Harats D. Dietary beta-carotene and alpha-tocopherol combination does not inhibit atherogenesis in an apoE-deficient mouse model. *Arterioscler Thromb Vasc Biol.* 1999;19:1470–1475.
36. Pratico D, Tangirala RK, Rader DJ, Rokach J, FitzGerald GA. Vitamin E suppresses isoprostane generation in vivo and reduces atherosclerosis in apoE-deficient mice. *Nat Med.* 1998;4:1189–1192.
37. Crawford RS, Kirk EA, Rosenfeld ME, LeBoeuf RC, Chait A. Dietary antioxidants inhibit development of fatty streak lesions in the LDL receptor-deficient mouse. *Arterioscler Thromb Vasc Biol.* 1998;18: 1506–1513.
38. Bird DA, Tangirala RK, Fruebis J, Steinberg D, Witztum JL, Palinski W. Effect of probucol on LDL oxidation and atherosclerosis in LDL receptor-deficient mice. *J Lipid Res.* 1998;39:1079–1090.
39. Li AC, Brown KK, Silvestre MJ, Willson TM, Palinski W, Glass CK. Peroxisome proliferator-activated receptor gamma ligands inhibit development of atherosclerosis in LDL receptor-deficient mice. *J Clin Invest.* 2000;106:523–531.
40. Yusuf S, Dagenais G, Pogue J, Bosch J, Sleight P. Vitamin E supplementation and cardiovascular events in high-risk patients: the Heart Outcomes Prevention Evaluation Study Investigators. *N Engl J Med.* 2000;342:154–160.